

Fermion exchange interaction between magnetic Skyrmions

I. Perapechka

Belarusian State University, Minsk 220004, Belarus

Ya. Shnir

*BLTP, JINR, Dubna 141980, Moscow Region, Russia Department of Theoretical Physics,
Tomsk State Pedagogical University, Russia*

(Received 3 February 2019; published 3 June 2019)

We propose a new mechanism of exchange interaction between the solitons related with the presence of localized fermions. Since the Atiyah-Patodi-Singer index theorem implies that such modes always exist for any topological soliton, their appearance may significantly alter the usual pattern of interaction. We elaborate this possibility considering, as a particular example, the chiral magnetic skyrmions coupled to spin-isospin fermions. It is shown that there are sequences of fermionic modes localized on the skyrmions. We investigate the additional effect of exchange interaction between the solitons with localized fermionic modes and demonstrate the existence of a stable system of magnetic skyrmions bounded by the strong attractive interaction mediated by the chargeless fermions.

DOI: [10.1103/PhysRevD.99.125001](https://doi.org/10.1103/PhysRevD.99.125001)

I. INTRODUCTION

Since the discovery of the solitons in the early 1960s, these particlelike configurations have been intensively studied in various frameworks in a wide variety of physical systems. Solitons are relevant to numerous areas of physics; they naturally arise in condensed matter physics, classical and quantum field theories, cosmology, biology, nuclear physics, and other disciplines. In many cases existence of the solitons is related with topological properties of the system; such solutions are absolutely stable against perturbations; see, e.g., [1,2].

The Skyrme model [3] is a prototype example of a theory that supports topological solitons, the skyrmions. It was first proposed around the 1960s to describe the nucleons. Later, it was shown by Witten [4] that the Skyrme model can be considered as a low energy effective theory of pion mean field.

An interesting new development in the application of the Skyrme model is related with its simplified 2 + 1-dimensional analogue, the so-called baby-Skyrme model [5–7]. This model finds various physical realizations; for example, planar skyrmions occur in the description of the quantum Hall effect [8,9]; such a model also arises in the description of ferromagnetic structures with Dzyaloshinskii-Moriya (DM) interaction [10,11], or in chiral nematic and

anisotropic fluids [12,13]. Very recently, there has been rapidly increasing interest both in the theoretical and experimental study of magnetic skyrmions, because of their possible use in future magnetic storage devices; see [14].

A peculiar property of topological solitons is the link between the topological charge of the configuration and the number of quasizero fermionic modes localized on the soliton. The Atiyah-Patodi-Singer index theorem [15] yields a remarkable relation between these quantities.¹ In particular, we can expect the existence of the fermionic modes confined by a magnetic skyrmion. These modes may represent the surface states of a three-dimensional topological insulator that become localized on the skyrmions [17,18]. More generally, the presence of localized fermions may affect the usual pattern of interaction between the solitons providing an additional exchange interaction. Notably, such a mechanism of fermion exchange interaction is not restricted to the particular case of the planar skyrmions; it is a general feature of any system of topological solitons with localized quasizero fermionic modes. On the other hand, analysis of the magnetic skyrmions with localized fermions is of particular interest because it was argued that this effect may lead to a new mechanism of nonconventional superconductivity in two-dimensional systems [19–21].

Properties of magnetic skyrmions in the model with the DM interaction term strongly depends on the explicit structure of the energy functional with magnetocrystalline

Published by the American Physical Society under the terms of the Creative Commons Attribution 4.0 International license. Further distribution of this work must maintain attribution to the author(s) and the published article's title, journal citation, and DOI. Funded by SCOAP³.

¹A simple formulation of the index theorem for the topological insulators is given in [16].

anisotropy; it may provide both repulsive and attractive interactions [22,23]. However, the Bloch-type skyrmions always repel each other; there is no multisoliton solution in such a system [24]. Thus, this model provides a nice framework for studying the effects caused by an additional exchange interaction mediated by the localized fermions.

Note that in consideration of the fermion-skyrmion system one must properly take into account the symmetries of the DM interaction term. A detailed analysis of the problem is yet missing. It remains a challenge to find a complete set of solutions of the corresponding full system of dynamical equations, especially for multisoliton configurations, which do not possess rotational invariance.

A main objective of this paper is to examine this system consistently, taking into account the backreaction of the fermions. In our numerical simulations we find the spectrum of the corresponding Hamiltonian and show that, indeed, there are various spin-isospin fermionic modes localized on a chiral magnetic skyrmion. Here we show, for the first time to our knowledge, that these modes give rise to additional attractive interaction between the solitons, which form bounded states.

II. THE MODEL

The Hamiltonian of a chiral magnetic planar system with a violation of the inversion symmetry and a strong spin-orbit coupling of the compound is

$$\mathcal{H}_s = \frac{J}{2} (\nabla \boldsymbol{\phi})^2 + D \boldsymbol{\phi} \cdot (\nabla \times \boldsymbol{\phi}) - \mathbf{B} \cdot \boldsymbol{\phi}. \quad (1)$$

These three terms correspond to the Heisenberg interaction, the DM interaction energy, and the symmetry breaking Zeeman energy of the interaction with an external magnetic field $\mathbf{B} = B \hat{\mathbf{z}}$, respectively. Here J is the magnetic stiffness constant and D is the strength of the DM interaction. The magnetization vector $\boldsymbol{\phi}$ is constrained to the surface of the unit sphere: $\boldsymbol{\phi} \cdot \boldsymbol{\phi} = 1$. Since on the boundary the magnetization vector is directed along the external magnetic field, $\boldsymbol{\phi}_\infty = (0, 0, 1)$, the field $\boldsymbol{\phi}$ is the map S^2 to S^2 . The corresponding topological invariant is $Q = -\frac{1}{4\pi} \int \boldsymbol{\phi} \cdot (\partial_x \boldsymbol{\phi} \times \partial_y \boldsymbol{\phi}) dx dy$; see, e.g., [1,2].

Note that the DM interaction breaks the spatial and internal O(2) symmetries of the model to the diagonal subgroup; the spatial rotations of the configuration yield its internal rotations and visa versa. Therefore the fermion field Ψ coupled to the magnetic skyrmion must be a spin-isospin spinor; the corresponding Lagrangian is

$$\mathcal{H}_f = \Psi^\dagger \hat{\gamma}^3 (-i \hat{\gamma}^k \partial_k + e \hat{\gamma}^k A_k + m + g \boldsymbol{\tau} \cdot \boldsymbol{\phi}) \Psi. \quad (2)$$

The isospin matrices are defined as $\boldsymbol{\tau} = \mathbb{I} \otimes \boldsymbol{\sigma}$, whereas the spin matrices are $\hat{\gamma}_\mu = \gamma_\mu \otimes \mathbb{I}$ where $\gamma_1 = -i\sigma_1, \gamma_2 = -i\sigma_2$ and $\gamma_3 = \sigma_3$, \mathbb{I} is two-dimensional identity matrix, $\hat{\partial} = \hat{\gamma}_\mu \partial^\mu$, and $\boldsymbol{\sigma}$ are the usual Pauli matrices. The last term in (2) represents the Hund coupling; the constant g

parametrizes the strength of the fermion-skyrmion interaction, m is the fermion mass, and e is the electromagnetic coupling. The vector potential of the external magnetic field is $A_\mu = \frac{B}{2}(0, -y, x)$. The total Hamiltonian of the coupled system $H = H_s + H_f$ depends on six parameters, J, D, B, g, m , and e . An appropriate rescaling of the coordinates, fields, and coupling constants allows us to reduce the number of independent parameters to three: g, m , and e . However, for the sake of clarity, we also keep the magnetic field B as a parameter although in our numerical simulations we have set it to 0.1.

Hereafter we consider stationary configurations, $\boldsymbol{\phi} = \boldsymbol{\phi}(x^k), \Psi = \psi(x^k) e^{-i\epsilon t}$. The corresponding equation for the fermionic eigenfunctions is

$$\hat{\gamma}^3 (-i \hat{\gamma}^k \partial_k + e \hat{\gamma}^k A_k + m + g \boldsymbol{\tau} \cdot \boldsymbol{\phi}) \psi = \epsilon \psi; \quad (3)$$

thus, the eigenvalues ϵ correspond to the energy of the fermions. Further, the equation for the field $\boldsymbol{\phi}$ is

$$\Delta \boldsymbol{\phi} - 2 \nabla \times \boldsymbol{\phi} + \mathbf{B} - g \psi^\dagger \hat{\gamma}_3 \boldsymbol{\tau} \psi = 0. \quad (4)$$

Note that we neither impose the usual assumption that $\boldsymbol{\phi}$ is a fixed static background field, nor make an approximation of its profile.

The complete system of coupled equations (3) and (4) must be solved numerically. This task can be simplified if we take into account the symmetry properties of this system. Note that it enjoys the following discrete symmetries:

$$\begin{aligned} x \rightarrow -x, & \quad \phi_y \rightarrow -\phi_y, & \quad \psi \rightarrow \hat{\gamma}^3 \psi^*, & \quad \epsilon \rightarrow -\epsilon; \\ y \rightarrow -y, & \quad \phi_x \rightarrow -\phi_x, & \quad \psi \rightarrow \tau_3 \psi^*, & \quad \epsilon \rightarrow -\epsilon. \end{aligned} \quad (5)$$

In the limiting case of massless uncharged fermions with $m = e = 0$ the system (3) and (4) is enhanced by additional symmetry of the fermion field $\psi \rightarrow -i\sigma_2 \otimes \sigma_2 \psi^*, \epsilon \rightarrow -\epsilon$.

First, we consider the O(2) invariant configuration, which is parametrized by the ansatz,

$$\boldsymbol{\phi} = (\sin f(r) \cos(n\varphi + \delta), \sin f(r) \sin(n\varphi + \delta), \cos f(r)). \quad (6)$$

Here $f(r)$ is some monotonically decreasing radial function, φ is the azimuthal angle, $n \in \mathbb{Z}$, and the phase δ corresponds to the internal orientation of the soliton. Notably, the energy of the magnetic skyrmion depends on δ ; it is minimal for $\delta = \pi/2$; further, rotationally invariant configuration (6) exists only for $n = 1$ (helical Bloch skyrmions [14,24]). Since the field must approach the vacuum on the spatial asymptotic, it satisfies the boundary condition $\cos f(r) \rightarrow 1$ as $r \rightarrow \infty$, i.e., $f(\infty) \rightarrow 0$.

The fermionic Hamiltonian (2) can be written explicitly in the matrix form as

$$\mathcal{H}_f = \begin{pmatrix} g \cos f + m & -ige^{-in\varphi} \sin f & -e^{-i\varphi}(\partial_r - \frac{i\partial_\varphi}{r} + \frac{eBr}{2}) & 0 \\ ige^{in\varphi} \sin f & -g \cos f + m & 0 & -e^{-i\varphi}(\partial_r - \frac{i\partial_\varphi}{r} + \frac{eBr}{2}) \\ e^{i\varphi}(\partial_r + \frac{i\partial_\varphi}{r} - \frac{eBr}{2}) & 0 & -g \cos f - m & ige^{-in\varphi} \sin f \\ 0 & e^{i\varphi}(\partial_r + \frac{i\partial_\varphi}{r} - \frac{eBr}{2}) & -ige^{in\varphi} \sin f & g \cos f - m \end{pmatrix}. \quad (7)$$

The rotationally invariant fermionic Hamiltonian (2) commutes with the total angular momentum operator

$$K_3 = -i \frac{\partial}{\partial \varphi} + \frac{\hat{Y}_3}{2} + \frac{\tau_3}{2}. \quad (8)$$

The corresponding half-integer eigenvalues $\kappa = 1 + l$ can be used to classify different field configurations. The ground state corresponds to $\kappa = 0$ and thus $l = -1$.

Rotationally invariant spin-isospin eigenfunctions of the fermionic Hamiltonian (2) with the eigenvalues ε are

$$\psi = \mathcal{N} \begin{pmatrix} u_1 e^{il\varphi} \\ iu_2 e^{i(l+n)\varphi} \\ v_1 e^{i(l+1)\varphi} \\ iv_2 e^{i(l+n+1)\varphi} \end{pmatrix}, \quad (9)$$

where the components u_i and v_i are functions of the radial coordinate only, $l \in \mathbb{Z}$ is the angular momentum of the fermion, and \mathcal{N} is a normalization factor that is defined from the usual condition

$$\int d^2x \psi^\dagger \psi = 2\pi \mathcal{N}^2 \int_0^\infty r dr (v_1^2 + v_2^2 + u_1^2 + u_2^2) = 1.$$

Notably, there are localized modes among fermionic eigenfunctions (9). Indeed, substitution of the ansatz (6) into Eq. (4) yields

$$\begin{aligned} f'' + \frac{f'}{r} - \sin f \left(B + \frac{\cos f - 2r \sin f}{r^2} \right) \\ + g \sin f (u_1^2 + v_2^2 - u_2^2 - v_1^2) \\ + 2g \cos f (v_1 v_2 - u_1 u_2) = 0. \end{aligned}$$

Linearizing this equation in the asymptotic region, where both f and the fermionic field profile functions approach 0, we can see that

$$f'' + \frac{f'}{r} - f \left(B + \frac{1}{r^2} \right) = 0, \quad (10)$$

which is the usual modified Bessel equation, whose solution can be written in terms of the McDonald function, $f \sim K_1(r)$. Thus, as $r \rightarrow \infty$, we obtain

$$f \sim \frac{e^{-\sqrt{B}r}}{\sqrt{r}},$$

and the configuration is exponentially localized.

Considering fermions, we notice that in the limit of vanishing Hund coupling the system is reduced to the usual Dirac fermions in the uniform magnetic field. The energy spectrum of the charged fermions is given by the Landau levels

$$\varepsilon_k^2 = M^2 + B(|e|(2k+1) \pm e), \quad (11)$$

where $k \in \mathbb{Z}$. The levels are twofold degenerate (except $k = 0$); we can expect that this degeneration is lifted for a nonvanishing fermion-skyrmion coupling. The charged modes then become exponentially localized on the skyrmion; this effect gives rise to the electric charge of the configuration. Evidently, there is a long-range Coulomb electric interaction between two widely separated chiral skyrmions with fermionic modes localized on each of them.

For the chargeless modes ($e = 0$) the situation is different; this case is similar to that of the usual fermion-skyrmion system considered in [25]. Indeed, the asymptotic expansion of Eqs. (3) with parametrization (9) at $r \rightarrow \infty$ yields

$$\begin{aligned} u_1'' + \frac{u_1'}{r} - u_1 \left((g+m)^2 - \varepsilon^2 + \frac{l^2}{r^2} \right) &= 0, \\ u_2'' + \frac{u_2'}{r} - u_2 \left((g-m)^2 - \varepsilon^2 + \frac{(l+1)^2}{r^2} \right) &= 0, \\ v_1'' + \frac{v_1'}{r} - v_1 \left((g+m)^2 - \varepsilon^2 + \frac{(l+1)^2}{r^2} \right) &= 0, \\ v_2'' + \frac{v_2'}{r} - v_2 \left((g-m)^2 - \varepsilon^2 + \frac{(l+2)^2}{r^2} \right) &= 0. \end{aligned} \quad (12)$$

Thus, the components of the fermionic field decay as

$$\begin{aligned}
u_1 &\sim K_l(\sqrt{(g+m)^2 - \varepsilon^2 r}), \\
u_2 &\sim K_{l+1}(\sqrt{(g-m)^2 - \varepsilon^2 r}), \\
v_1 &\sim K_{l+1}(\sqrt{(g+m)^2 - \varepsilon^2 r}), \\
v_2 &\sim K_{l+2}(\sqrt{(g-m)^2 - \varepsilon^2 r}),
\end{aligned} \tag{13}$$

and the exponentially localized modes exist as $|\varepsilon| < g - m$.

III. NUMERICAL RESULTS

Equations (4) and (3), together with constraint imposed by the normalization condition, yield a system of integro-differential equations, which can be solved numerically. Generally, the system is not rotationally invariant and we impose an additional $O(3)$ constraint on the scalar field ϕ . We make use of the fourth order Newton-Raphson method implemented in the CESDSOL package; relative numerical errors are no higher than 10^{-5} .

First, we consider a rotationally invariant system of fermions coupled to the single skyrmion. The results for the fermionic energy spectrum are presented in Fig. 1. For the uncharged modes the general pattern is similar to what we found in our previous study of the fermions interacting with baby skyrmions [25]. In agreement with the index theorem, for a given value of l , there is one zero-crossing mode that runs from negative to positive as the Hund coupling g is increasing. Apart from this mode there are localized states of two different types, which are linked to the negative and positive continuum. We refer to them as the modes of types A and B , respectively.

The spectral flow of the charged fermions is different; see Fig. 1, right plot. In the limiting case $g = 0$ the fermions are decoupled from the skyrmion; they occupy the Landau

levels (11). For each value of $l \neq 0$ there are two modes on each level; the zero mode corresponds to $k = 0$, $l = -1$. As the Hund coupling g increases, the states start to deform; the energy of the lowest mode becomes negative, and it has a minimum at some value of g . As the coupling increases further, the energy of the lowest mode is increasing; it crosses 0 at some critical value of the Hund coupling. This mode remains localized on the skyrmion for all values of the coupling, while other charged modes with $k \neq 0$ are linked to the positive or negative energy continuum, approaching it at some set of critical values of the fermion-skyrmion coupling g . Further, as g increases, the fermion-skyrmion interaction becomes stronger than the interaction between the fermions and magnetic field \mathbf{B} ; thus there is a one-to-one correspondence between the corresponding localized modes and the uncharged modes of the types A_k and B_k .

Localization of the fermionic modes may strongly affect the usual pattern of interaction between the magnetic skyrmions. Notably, even chargeless fermionic modes may balance the repulsive interaction between the chiral skyrmions.

In order to evaluate the potential of the fermion exchange interaction between the solitons, we can make use of the product ansatz [1] adopted for planar skyrmions. The field of a skyrmion ϕ can be reexpressed via $SU(2)$ valued Hermitian matrix fields $U = \phi \cdot \boldsymbol{\tau}$; thus the field of two well-separated skyrmions can be reasonably approximated by $U_1(\mathbf{x})U_2(\mathbf{x})$.

Calculating the fermion spectrum on such a background, we can find the potential of interaction between the skyrmions, mediated by a single chargeless fermionic mode A_0 ; see Fig. 2. The energy of interaction of two skyrmions in such a system can be evaluated as $E_{\text{int}} = E - 2M - \varepsilon_\infty$, where E is the total energy of the

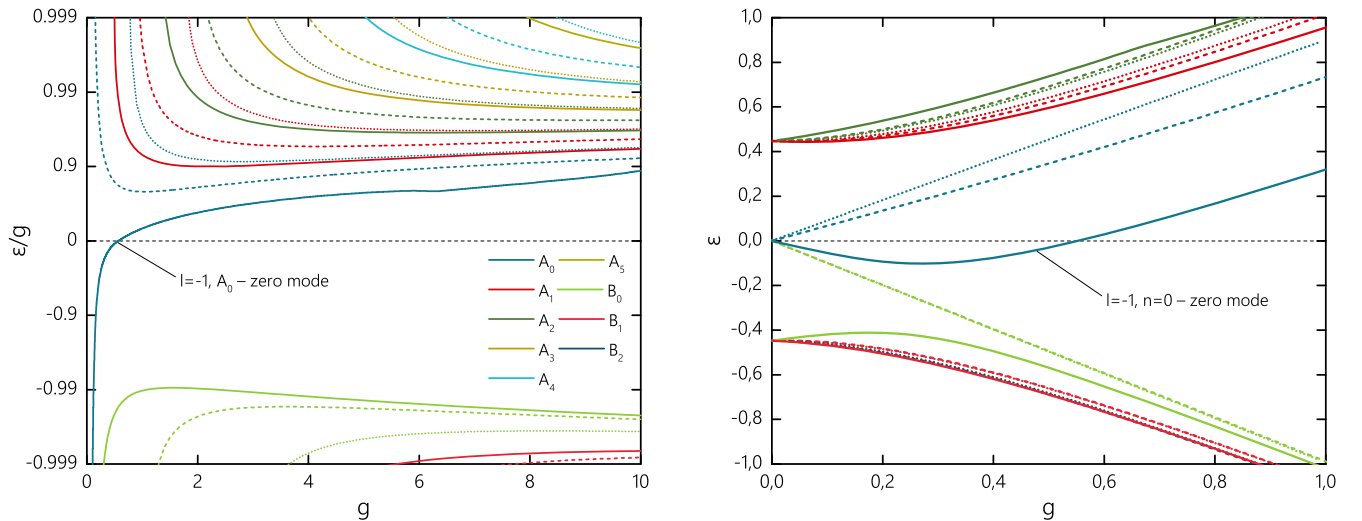


FIG. 1. Energy ε of the chargeless ($e = 0$, left plot) and charged ($e = -1$, right plot) localized massless fermions as a function of the coupling constant g . The solid, dashed, and dotted lines correspond to $l = -1, 0, 1$, respectively.

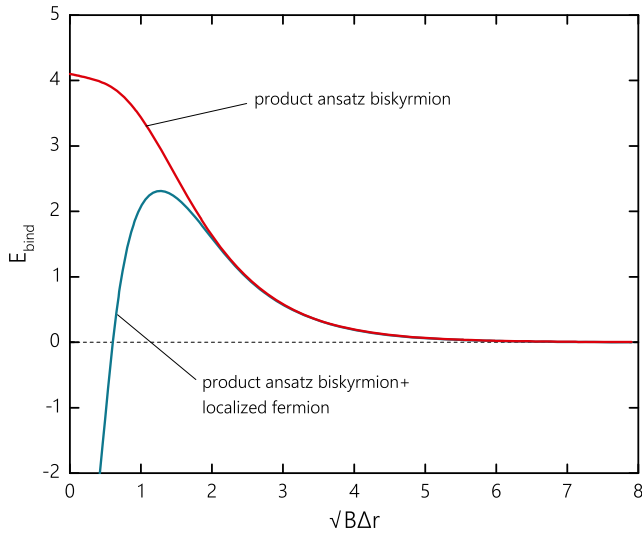


FIG. 2. Interaction potential of two skyrmions in the presence of the localized fermionic mode A_0 at $g = 5$ and $g = 0$.

biskyrmion-fermion configuration, M is the mass of a single skyrmion, and ε_∞ is the energy of the fermion localized on widely separated skyrmions. Clearly, the interaction potential possesses a minimum at zero separation for a nonvanishing coupling g . Thus, we may expect that the bounded multiskyrmion configurations may exist in the presence of localized fermionic modes. Note that the position of the minimum of the evaluated interaction potential is related with restrictions, imposed by the product ansatz. The situation changes as the backreaction of the fermions is taken into account.

Full numerical solution of the system of coupled equations (3) and (4) without restrictions of symmetry shows that biskyrmion-fermion configurations exist for

relatively large values of the coupling g ; moreover, several branches of solutions and different configurations may exist for the same value of g . All solutions we found satisfy the symmetry restrictions (5).

In Fig. 3 we display the fermion energy (in units of g) and interaction energy E_{int} as functions of the coupling strength g . First, we observe that the bounded system of two charge one skyrmions with a localized A_0 mode appears as a local minimum as g increases above $g_{cr}^{(1)} = 2.17$; see the left plots in Fig. 4. The bounded solutions do not exist as $g < g_{cr}^{(1)}$. As the Hund coupling increases, the overlap becomes stronger and the solitons approach each other. The energy of the fermionic mode is increasing; it crosses zero and the energy of interaction becomes negative, although both skyrmions remain separated, as shown in plots 2, Fig. 4. This branch of solutions terminates at some upper critical value of the coupling $g_{cr}^{(2)} \approx 5.22$; here it bifurcates with the second branch, which extends backwards as the coupling g is decreasing. Along this branch the maximum of the fermionic density distribution is located at the center of the elongated soliton configuration; see plots 4 in Fig. 4. The energy of the fermionic mode is decreasing as g decreases; in accordance with the index theorem it crosses 0 for a second time and tends towards the negative continuum as the solitons approach closer to each other. At some lower critical value $g_{cr}^{(3)} \approx 0.75$ this branch bifurcates with another one, along which solitons merge forming an almost rotationally invariant configuration of topological degree 2; see plots 5, Fig. 4.

Along the corresponding third branch the coupling becomes stronger. No indication is found for termination of this branch; it exists for arbitrary large values of the coupling.

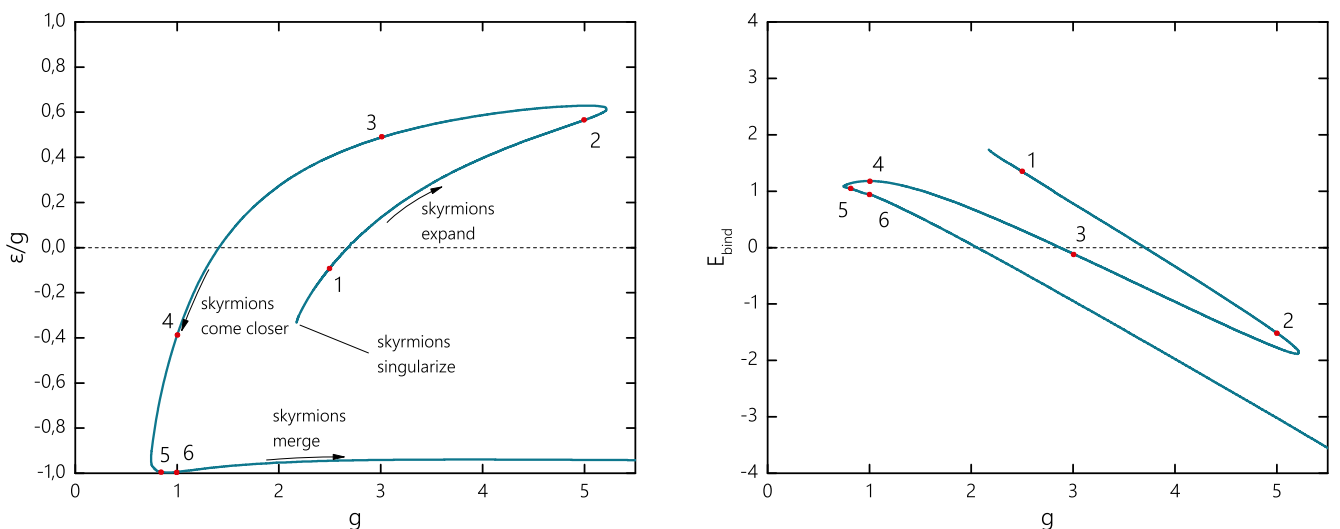


FIG. 3. Normalized energy ε/g (left plot) of the chargeless massless fermionic mode and the interaction energy E_{int} (right plot) of the biskyrmion with the localized mode as a function of the coupling g . The numbers on the curves correspond to the plots in Fig. 4.

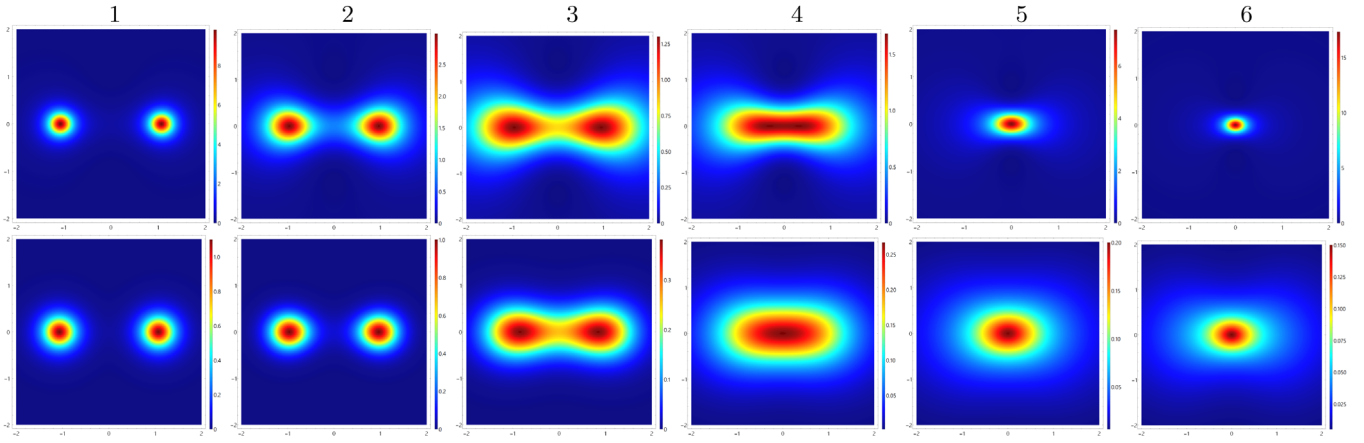


FIG. 4. Biskyrmion-fermion bounded system: density plots of the distributions of the topological charge density (upper row) and the fermionic density (bottom row). The plot numbers correspond to the values of the coupling constants marked as dots in Fig. 3.

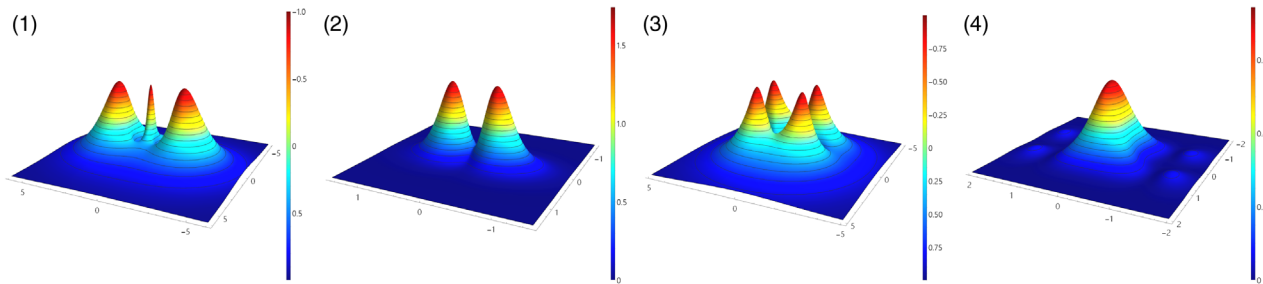


FIG. 5. Multiskyrmion-fermion bounded systems: Field components ϕ_3 of the $Q = 3$ and $Q = 4$ magnetic Skyrmions (plots 1 and 3, respectively) and the corresponding fermionic density distributions (plots 2 and 4, respectively) at $g = 5$.

Furthermore, we found other multisoliton configurations bounded by the fermionic modes. In Fig. 5, as particular examples, we display the solutions we found in sectors of degrees $Q = 3, 4$; there is an interesting pattern of transformations of the configurations as the Hund coupling varies.

Our investigation has shown that the localization of the spin-isospin fermionic modes on the magnetic chiral skyrmions with DM interaction strongly affects the usual picture of repulsive interaction between the Bloch skyrmions. The new mechanism enabling bound multisoliton solutions to occur is the fermionic exchange interaction mediated by the localized spin-isospin fermions. Since the index theorem secures existence of similar modes for any topological soliton, we expect similar bounded multisoliton solutions may exist in many different systems, for example, in the conventional baby-Skyrme model coupled with

fermions, as well as in various higher dimensional models, like the Abelian Higgs model or Yang-Mills theory. We hope to address these problems in our future work.

ACKNOWLEDGMENTS

We are grateful to Steffen Krusch, Nobuyuki Sawado, and Paul Sutcliffe for helpful discussions. The authors acknowledge support by the DAAD Ostpartnerschaft Programm. Ya. S. gratefully acknowledges the support of the Alexander von Humboldt Foundation and from the Ministry of Education and Science of Russian Federation, Grant No. 3.1386.2017. We thank Jutta Kunz for kind hospitality at the Department of Physics, Carl von Ossietzky University of Oldenburg during the completion of this work.

[1] N. S. Manton and P. Sutcliffe, *Topological Solitons* (Cambridge University Press, Cambridge, England, 2004).

[2] Y. M. Shnir, *Topological and nonTopological Solitons in Scalar Field Theories* (Cambridge University Press, Cambridge, England, 2018).

- [3] T. H. R. Skyrme, *Proc. R. Soc. A* **260**, 127 (1961).
- [4] E. Witten, *Nucl. Phys.* **B223**, 422 (1983).
- [5] A. A. Bogolubskaya and I. L. Bogolubsky, *Phys. Lett. A* **136**, 485 (1989).
- [6] R. A. Leese, M. Peyrard, and W. J. Zakrzewski, *Nonlinearity* **3**, 773 (1990).
- [7] B. M. A. G. Piette, B. J. Schroers, and W. J. Zakrzewski, *Z. Phys. C* **65**, 165 (1995).
- [8] A. Schmeller, J. P. Eisenstein, L. N. Pfeiffer, and K. W. West, *Phys. Rev. Lett.* **75**, 4290 (1995).
- [9] D. H. Lee and C. L. Kane, *Phys. Rev. Lett.* **64**, 1313 (1990).
- [10] A. N. Bogdanov and D. A. Yablonsky, *Sov. Phys. JETP* **95**, 178 (1989); A. N. Bogdanov, *JETP Lett.* **62**, 247 (1995).
- [11] S. Mühlbauer, B. Binz, F. Jonietz, C. Pfleiderer, A. Rosch, A. Neubauer, R. Georgii, and P. Boni, *Science* **323**, 915 (2009); X. Z. Yu, Y. Onose, N. Kanazawa, J. H. Park, J. H. Han, Y. Matsui, N. Nagaosa, and Y. Tokura, *Nature (London)* **465**, 901 (2010).
- [12] I. I. Smalyukh, Y. Lansac, N. A. Clark, and R. P. Trivedi, *Nat. Mater.* **9**, 139 (2010).
- [13] P. J. Ackerman, R. P. Trivedi, B. Senyuk, J. van de Lagemaat, and I. I. Smalyukh, *Phys. Rev. E* **90**, 012505 (2014).
- [14] N. Nagaosa and Y. Tokura, *Nat. Nanotechnol.* **8**, 899 (2013).
- [15] M. F. Atiyah, V. K. Patodi, and I. M. Singer, *Math. Proc. Cambridge Philos. Soc.* **77**, 43 (1975).
- [16] H. Fukaya, T. Onogi, and S. Yamaguchi, *EPJ Web Conf.* **175**, 11009 (2018).
- [17] H. M. Hurst, D. K. Efimkin, J. Zang, and V. Galitski, *Phys. Rev. B* **91**, 060401 (2015).
- [18] D. Andrikopoulos, B. Sorée, and J. De Boeck, *J. Appl. Phys.* **119**, 193903 (2016).
- [19] G. Baskaran, arXiv:1108.3562.
- [20] C. K. Lu and I. F. Herbut, *Phys. Rev. Lett.* **108**, 266402 (2012).
- [21] A. Knigavko, B. Rosenstein, and Y. F. Chen, *Phys. Rev. B* **60**, 550 (1999).
- [22] J. C. Loudon, A. O. Leonov, A. N. Bogdanov, M. C. Hatnean, and G. Balakrishnan, *Phys. Rev. B* **97**, 134403 (2018).
- [23] H. Du, X. Zhao *et al.*, *Phys. Rev. Lett.* **120**, 197203 (2018).
- [24] *skyrmions: Topological Structures, Properties, and Applications*, edited by J. P. Liu, Z. Zhidong, and Z. Guoping (CRC Press, London, 2016).
- [25] I. Perapechka, N. Sawado, and Y. Shnir, *J. High Energy Phys.* **10** (2018) 081.